Cholesterol in mouse retina originates primarily from in situ de novo biosynthesis

Joseph B. Lin,* Natalia Mast,* Ilya R. Bederman,† Yong Li,* Henri Brunengraber,§ Ingemar Björkhem, and Irina A. Pikuleva[1,*]**

Department of Ophthalmology and Visual Sciences,* Department of Pediatrics,† and Department of Nutrition,§ Case Western Reserve University, Cleveland, OH 44106; and Division of Clinical Chemistry, Department of Laboratory Medicine,** Karolinska University Hospital, Karolinska Institute, Huddinge, Stockholm 141 86 Sweden

Abstract The retina, a thin tissue in the back of the eye, has two apparent sources of cholesterol: in situ biosynthesis and cholesterol available from the systemic circulation. The quantitative contributions of these two cholesterol sources to the retinal cholesterol pool are unknown and have been determined in the present work. A new methodology was used. Mice were given separately deuterium-labeled drinking water and chow containing 0.3% deuterium-labeled cholesterol. In the retina, the rate of total cholesterol input was 21 μg of cholesterol/g retina • day, of which 15 μg of cholesterol/g retina • day was provided by local biosynthesis and 6 μg of cholesterol/g retina • day was uptaken from the systemic circulation. Thus, local cholesterol biosynthesis accounts for the majority (72%) of retinal cholesterol input. We also quantified cholesterol input to mouse brain, the organ sharing important similarities with the retina. The rate of total cerebral cholesterol input was 121 μg of cholesterol/g brain • day with local biosynthesis providing 97% of total cholesterol input. Our work addresses a long-standing question in eye research and adds new knowledge to the potential use of statins (drugs that inhibit cholesterol biosynthesis) as therapeutics for age-related macular degeneration, a common blinding disease.—Lin, J. B., N. Mast, I. R. Bederman, Y. Li, H. Brunengraber, I. Björkhem, and I. A. Pikuleva. **Cholesterol in mouse retina originates primarily from in situ de novo biosynthesis. *J. Lipid Res.* 2016.** 57: **258–264.**

Supplementary key words dietary cholesterol • lipoproteins • low density lipoprotein • mass spectrometry • brain lipids • cholesterol uptake • deuterium • age-related macular degeneration • isotopic tracer

Cholesterol is a ubiquitous lipid present in the retina (1), a light-sensitive tissue in the back of the eye that mediates the transmission of the visual signal to the brain. Cholesterol maintenance in the retina is still poorly understood but needs to be studied to delineate the link between retinal cholesterol and age-related macular degeneration (AMD) (2), a blinding disease affecting the elderly of the industrialized world (3).

The retina maintains cholesterol homeostasis by balancing cholesterol input and output (4). There are two known pathways of retinal cholesterol input: local cholesterol biosynthesis and tissue uptake of systemic cholesterol (i.e., cholesterol-containing lipoprotein particles from the systemic circulation) (5–9). The relative contributions, and thus significances, of these pathways to the retinal cholesterol pool are unknown, ultimately impeding the prioritization of research directions in studies of retinal cholesterol (2).

In the present work, we capitalized on the methodological approach developed in our previous investigation of cholesterol input to the brain of mice with disrupted blood-brain barrier (10). This approach is based on the measurement of the rate of total tissue cholesterol input by administering deuterated water to mice. The rate of tissue uptake of systemic cholesterol is then determined in a separate experiment by feeding mice ^{2}H-labeled cholesterol. The difference between the two rates can be calculated and represents the rate of tissue cholesterol biosynthesis. We applied our approach to the quantification of cholesterol input to mouse retina and, for comparison, characterized cholesterol input to normal mouse brain, which is also a part of the central nervous system. Both the retina and brain contain neurons and glial cells and are separated from the systemic circulation by the blood-retinal

This work was supported in part by National Institutes of Health Grant R01 EY018383 (I.A.P.), a Fellowship for Summer Undergraduate Research from the American Society for Pharmacology and Experimental Therapeutics (J.B.L.), an unrestricted grant from Research to Prevent Blindness, Core Facility P30 Grant EY11373, and grants from the Swedish Research Council and Swedish Brain Power (I.B.). I.A.P. is a Carl F. Asseff Professor of Ophthalmology. The contents are solely the responsibility of the authors and do not necessarily represent the official views of the National Institutes of Health.

Manuscript received 9 October 2015 and in revised form 30 November 2015.

Published, JLR Papers in Press, December 2, 2015
DOI 10.1194/jlr.M064469

Abbreviations: AMD, age-related macular degeneration; [$^{2}H_7$]β-sitosterol, [25,26,26,26,27,27,27-$^{2}H_7$]β-sitosterol; [$^{2}H_7$]cholesterol, [25,26,26,26,27,27,27-$^{2}H_7$]cholesterol.

[1]To whom correspondence should be addressed.
e-mail: iap8@case.edu

barrier and blood-brain barrier, respectively. The blood-retinal barrier is permeable to cholesterol; therefore, the retina has two pathways of cholesterol input. In contrast, the blood-brain barrier is impermeable to cholesterol, the reason why in situ biosynthesis is essentially the only pathway of cholesterol input to the brain (11). The present work established that in situ biosynthesis is the major source of cholesterol for both the retina and brain and identified the quantitative differences between retinal and brain cholesterol input. The data obtained fill a fundamental gap in our knowledge of retinal cholesterol maintenance and will facilitate the development of pharmacologic treatments for ocular diseases associated with deleterious accumulations of retinal cholesterol.

MATERIALS AND METHODS

Materials

[25,26,26,26,27,27,27-$^2H_7$]cholesterol ([$^2H_7$]cholesterol) was purchased from Cambridge Isotope Laboratories Inc., and [25,26,26,26,27,27,27-$^2H_7$]β-sitosterol ([$^2H_7$]β-sitosterol) was from Toronto Research Chemicals Inc. All other chemicals were purchased from Sigma-Aldrich. Regular rodent chow (5P75-5P76 Prolab Isopro RMH 3000) was from LabDiet and contained 0.02% cholesterol (w/w) and 5.0% fat (w/w). Diets containing 0.3% unlabeled cholesterol (w/w) and 15% fat (w/w) or 0.3% [$^2H_7$]cholesterol (w/w) and 15% fat (w/w) were prepared as described (12), except the chows were pelleted and food colors were added to facilitate diet identification. Briefly, 0.3 g of cholesterol was stirred into 9.7 g of peanut oil until cholesterol was dissolved. Cholesterol solution was added to 90 g of powdered rodent chow along with ~35 ml of water. All the components were thoroughly mixed for 30 min until a homogeneous dough was formed, which was then used for the manual preparation of pellets. The pellets were dried at 37°C overnight.

Animals

Animal studies were in compliance with the *Guide for Care and Use of Laboratory Animals* by the National Institutes of Health and approved by Case Western Reserve University's Animal Care and Use Committee. Female C57BL/6J mice (3–4 months old) were purchased from the Jackson Laboratory and housed in the Animal Resource Center at Case Western Reserve University. Animals were maintained in a standard 12 h light (~10 lux)/12 h dark cycle environment with water and food provided ad libitum.

Total tissue cholesterol input

Two groups of mice were used. One group (n = 9) was fed regular rodent chow for the whole duration of the experiment (**Fig. 1A**). This group was injected intraperitoneally with 0.5–0.8 ml ^2H_2O (equal to 3.5% of mouse body water) and kept on drinking water containing 6% ^2H_2O (v/v) for 9 h, 1 day, and 2 weeks prior to euthanasia. The other group of mice (n = 12) was put on the 0.3% cholesterol-containing diet 2 weeks prior to the experiment, then injected with ^2H_2O, and kept on the 0.3% cholesterol-containing diet and 6% ^2H-containing drinking water for 6 h, 1 day, 1 week, and 2 weeks before euthanasia.

Tissue uptake of dietary cholesterol

Mice (n = 5) were fed the 0.3% cholesterol-containing diet for 2 weeks and then switched to the 0.3% [$^2H_7$]cholesterol-containing diet, which was given for 1 week followed by animal euthanasia (**Fig. 2A**).

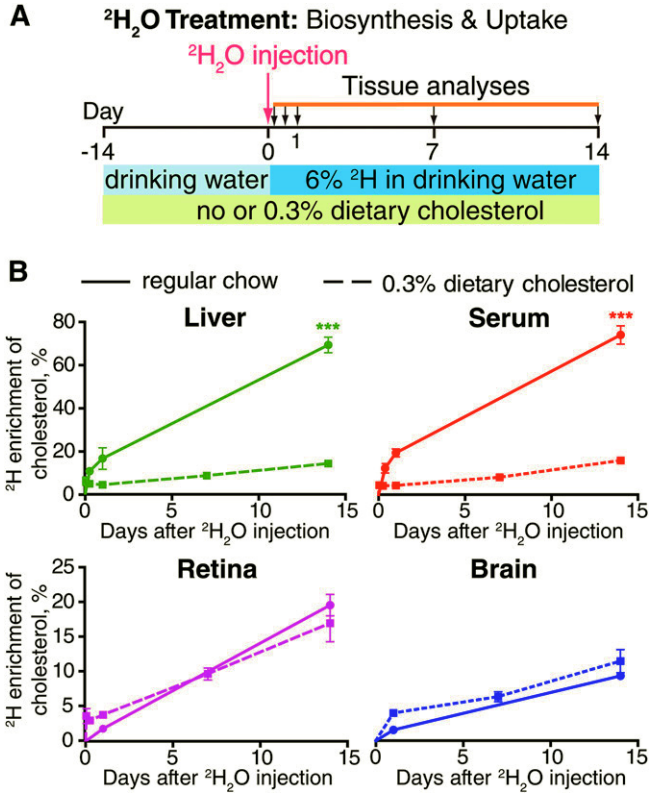

Fig. 1. Total tissue cholesterol input. A: Experimental paradigm. B: ^2H enrichment of cholesterol in each tissue. Each data point is the mean ± SD of measurements in individual (n = 3) mice. *** $P < 0.001$.

Tissue isolation and processing

Mice were anesthetized by an intraperitoneal injection of ketamine (80 mg/kg body weight) and xylazine (15 mg/kg body weight) at the end of the dark period of their light cycle (at ~8 AM) followed by the blood collection by cardiac puncture. Serum was prepared by keeping blood at room temperature for 30 min and pelleting the clot by centrifugation at 1,500 *g* for 10 min. Following blood collection, mice were perfused with 20 ml of phosphate buffer saline through the heart to remove residual blood from organs. The liver, brain, and retinas were isolated

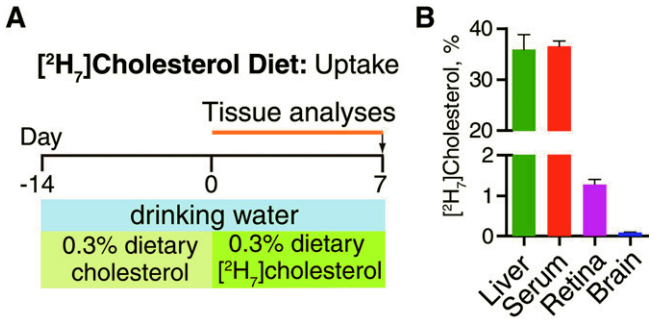

Fig. 2. Tissue uptake of dietary cholesterol. A: Experimental paradigm. B: Relative amount of [$^2H_7$]cholesterol in different tissues after 1-week treatment. Each bar is the mean ± SD of measurements in individual (n = 5) mice.

and processed as described (13). Briefly, after harvesting, organs were dipped quickly in cold phosphate buffer saline, blotted dry, and homogenized in 10 vol (w/v) of 50 mM potassium phosphate buffer (pH 7.2) containing 300 mM sucrose, 0.5 mM dithiothreitol, 10 mM EDTA, 100 μg/ml butylhydroxytoluene, and a cocktail of protease inhibitors. Cellular debris was removed by centrifugation at 1,500 *g* for 15 min, and protein concentration of the supernatant was determined by BCA Protein Assay Kit (Thermo Scientific). [$^2H_7$]β-sitosterol was added as an internal standard for cholesterol quantification: 60 nmol per 50 μl of serum, 50 nmol per mg of liver protein, 200 nmol per mg of brain protein, and 10 nmol per two retinas. Lipids were extracted by Folch, saponified, and derivatized with 100 μl of bis-(trimethylsilyl) trifluoroacetamide/trimethylchlorosilane (13). GC/MS analyses were conducted as described (13) by a 1 μl sample injection in split mode (1:12.5); in the case of retinal samples, 2 μl was injected.

Determination of body water (precursor) ^2H enrichment

This was carried out as described (14) by serum isotopic exchange with acetone. Briefly, 5 μl of serum from each animal was mixed with 5 μl of 10 N KOH and 5 μl of acetone in a GC/MS vial and incubated for 4 h at room temperature. A 1 μl sample of acetone vapor was then injected into the GC/MS system in split mode (1:10), and unlabeled and ^2H-labeled acetone were monitored by ion fragments *m/z* 58 and 59, respectively. The isotopic enrichment of acetone was calculated by the 59 / (58 + 59) *m/z* ratio and corrected to ^2H_2O enrichment using a calibration curve. This curve was prepared by mixing 5 μl of 0% to 10% ^2H_2O solutions with 5 μl of 10 N KOH and 5 μl of acetone and processing samples as described for serum.

GC/MS analyses

An Agilent 5973 Network Mass Selective Detector equipped with an Agilent 6890 Gas Chromatograph system and a ZB-5MS capillary column (60 m × 0.25 mm × 0.25 mm; Zebron, Charlotte, NC) was used. Gas chromatograph conditions for monitoring of cholesterol and acetone were as described (13, 15). Samples were analyzed in selected ion monitoring mode using electron impact ionization. Abundances for ion fragments were calculated by integrating the maximum peak heights.

Cholesterol quantifications

Calibration curves were generated using a fixed concentration of [$^2H_7$]β-sitosterol and varying concentrations of cholesterol or [$^2H_7$]cholesterol. Tissue cholesterol and [$^2H_7$]cholesterol were quantified based on the calibration curves by monitoring the ion fragments *m/z* 368, 375, and 364 for cholesterol, [$^2H_7$]cholesterol, and [$^2H_7$]β-sitosterol, respectively.

Calculations for ^2H cholesterol enrichment

These were carried out as described (16, 17) for the liver, serum, retina, and brain. Briefly, for each tissue, the cholesterol ion fragments *m/z* 368→373 were monitored and corrected for the background natural abundance of cholesterol mass isotopomers (18). The average number of ^2H atoms incorporated per cholesterol molecule was then calculated by $\sum m_i \times i$, where m_i is the fraction of cholesterol containing i (0 to 5) deuterons corresponding to ion fragments *m/z* 368→373. The data obtained were divided by the maximum number of deuterium atoms that can be incorporated into cholesterol ($N = 22$) (19) and each animal's precursor ^2H enrichment. The final values represented the percentage of ^2H cholesterol enrichment in individual tissues and reflected a sum of cholesterol biosynthesis and uptake of systemic cholesterol over a certain time period.

Calculations for tissue cholesterol uptake and biosynthesis rates

The rate of cholesterol uptake was calculated from the amont of [$^2H_7$]cholesterol present in each tissue after 1 week of dietary [$^2H_7$]cholesterol treatment using the following equation:

$$\text{Uptake per week, \%} = \left[{}^2H_7\right]\text{cholesterol in organ, \% /} \left(\left[{}^2H_7\right]\text{cholesterol in serum, \% / 100}\right)$$

Then, the rate of cholesterol biosynthesis was calculated based on the % uptake of systemic cholesterol and the data from a 1-week ^2H_2O experiment. The following equation was used:

$$\text{Biosynthesis per week, \%} = \text{total } {}^2H \text{ cholesterol enrichment in organ, \%} - (\text{uptake per week, \%} \times {}^2H \text{ enrichment of serum cholesterol, \% / 100})$$

Statistics

All data represent the means of the measurements in individual animals ± SD. The number of animals (n) was three per time point in the deuterated water experiments, and five mice in the dietary [$^2H_7$]cholesterol treatment. Statistical significance was assessed by the Student's two-tailed unpaired *t*-test using GraphPad Prism software.

RESULTS

Total tissue cholesterol input

Mice on two diets (regular rodent chow and cholesterol-containing diet) were characterized for the kinetics of appearance of ^2H in tissue cholesterol from the precursor ^2H_2O. Mice on regular rodent chow had very similar ^2H cholesterol enrichment in the liver and serum (Fig. 1B, solid green and solid red lines) indicating that nearly all cholesterol in mouse blood originates from the liver, consistent with findings in rats (20). Also, the liver and serum showed similar decreases in ^2H cholesterol enrichment under the cholesterol-containing diet (Fig. 1B, dashed green and dashed red lines). At 2 weeks postinjection with ^2H_2O, these decreases were from 69 ± 4% to 14 ± 1% in the liver and from 74 ± 4% to 16 ± 1% in the serum. These changes in ^2H enrichment reflect the known suppression of hepatic cholesterol biosynthesis in rodents when they are fed a cholesterol-containing diet (21). Compensatory reduction of hepatic cholesterol biosynthesis is a reason why mice are resistant to atherosclerosis when challenged with a high-cholesterol diet (22).

^2H cholesterol enrichments in the retina and brain were lower than those in the liver and serum and showed essentially no response to cholesterol-containing chow (Fig. 1B, purple and blue solid and dashed lines). When fed regular rodent chow, ^2H cholesterol enrichment was 20 ± 2% and 9 ± 1% in the retina and brain, respectively, at 2 weeks postinjection with ^2H_2O. When fed the cholesterol-containing diet, ^2H cholesterol enrichment was 17 ± 3% in the retina and 11 ± 2% in the brain, statistically insignificant changes relative to enrichment measured in animals fed

regular rodent chow. Similarly, the cholesterol-containing diet had no effect on retinal and brain cholesterol content, which remained unchanged and equal to 1.13 ± 0.08 mg/g retina and 13 ± 1 mg/g brain (**Table 1**, line 6). Little to no effect of dietary cholesterol on ^{2}H cholesterol enrichment in the retina was the first indication that local biosynthesis is the predominant pathway of cholesterol input to mouse retina.

Tissue uptake of dietary cholesterol

Feeding mice the 0.3% [$^2H_7$]cholesterol-containing diet for 1 week led to the appearance of 35.9 ± 2.9% of [$^2H_7$] cholesterol in the liver, 36.5 ± 1.1% in the serum, 1.3 ± 0.1% in the retina, and 0.09 ± 0.01% in the brain (Fig. 2B). The negligible amount of tracer cholesterol in the brain was also observed in previous studies (10, 11).

Cholesterol uptake and biosynthesis rates

To calculate these rates, we first divided the percentages of [$^2H_7$]cholesterol in retina and brain after a 1-week treatment with the [$^2H_7$]cholesterol-containing diet by the fractional enrichment of [$^2H_7$]cholesterol in the serum after the same period of time (Table 1, line 1). This yielded the percent of cholesterol uptake per week (Table 1, line 2). The values obtained (3.6% in the retina and 0.2% in the brain) were then multiplied by ^{2}H cholesterol enrichment in the serum from the deuterated water experiment at 1 week. Next, these products (Table 1, line 3) were subtracted from the total amount of ^{2}H cholesterol enrichment in the retina and brain (Table 1, line 4), thus providing the percent of cholesterol biosynthesis per week (Table 1, line 5). The subtraction of line 3 from line 4 was based on the assumption that retinal uptake of systemic cholesterol synthesized endogenously by extraocular organs is the same or very similar to that of systemic cholesterol containing a fraction of dietary cholesterol. Indeed, when mice are challenged with a cholesterol-containing diet, they not only have a compensatory reduction of hepatic cholesterol biosynthesis (22), but also tightly control intermediate- and low-density cholesterol in the serum (23). Consistent with these homeostatic responses, serum cholesterol in our study was similar in mice on regular rodent chow and animals on 0.3% dietary cholesterol (50 ± 10 mg/dl). Hence, we did not measure serum lipoprotein profiles, especially when there are studies by others demonstrating that a 30-day mouse feeding with a much higher, 2%, cholesterol-containing diet does not alter their plasma lipoprotein profiles (23). Our data analysis was finished by multiplying line 5 (Table 1) by the cholesterol content per gram of wet tissue (Table 1, line 6) to obtain absolute values of cholesterol input rates (Table 1, lines 8, 9), and the calculation of the relative rates of the individual pathways of cholesterol input to compare the retina and brain (Table 1, lines 11, 12).

We found that the rates of cholesterol biosynthesis were 15 μg/g retina • day (or 9.4% per week) and 117 μg/g brain • day (or 6.3% per week) (Table 1, lines 8, 11). The rates of uptake of systemic cholesterol were lower and equal to 6 μg/g retina • day (or 3.6% per week) and 4 μg/g brain • day (or 0.2% per week) (Table 1, lines 9, 12). Thus, 72% of cholesterol in mouse retina originates from local biosynthesis, and 28% is obtained from uptake of blood-borne cholesterol (Table 1, line 11). In the brain, nearly all of cholesterol input is achieved via local biosynthesis (97%) because the blood-brain barrier is impermeable to cholesterol (24). The 3% of cholesterol input from circulation must be a maximum value because it was calculated from the 0.1% of [$^2H_7$]cholesterol enrichment in the brain after 1 week of treatment with dietary [$^2H_7$]cholesterol. These trace amounts of [$^2H_7$]cholesterol could represent contamination with blood-borne cholesterol because our previous study showed that these small amounts of deuterated brain cholesterol did not increase as the treatment time with dietary deuterated cholesterol increased (10).

Cholesterol turnover times

Under steady-state conditions, cholesterol input equals cholesterol output. Hence, if 0.021 mg of cholesterol is provided to the retina per gram wet tissue • day (Table 1, line 7), and retinal cholesterol content is 1.13 mg

TABLE 1. Calculations for cholesterol biosynthesis and uptake rates for mouse retina and brain

Line #	Experimental Data/Calculated Values	Serum	Retina	Brain
	Mice exposure to dietary [$^2H_7$]cholesterol			
1	*[$^2H_7$]cholesterol, %*	*36.5 ± 1.1*	*1.3 ± 0.1*	*0.09 ± 0.01*
2	**Cholesterol uptake per week, %**	**ND**	**3.6**	**0.2**
	Mice exposure to deuterated water			
3	^{2}H cholesterol enrichment originating from uptake, %	ND	0.29	0.02
4	*Total ^{2}H cholesterol enrichment, %*	*8.1 ± 1.0*	*9.7 ± 0.9*	*6.3 ± 0.7*
5	**Cholesterol biosynthesis per week, %**	**ND**	**9.4**	**6.3**
	Summary data			
6	*Cholesterol content, mg/g wet tissue*	*ND*	*1.13 ± 0.08*	*13 ± 1*
7	Absolute rate of cholesterol input, μg/g wet tissue • day	ND	21	121
8	Local biosynthesis	ND	15	117
9	Uptake from blood	ND	6	4
10	Relative rate of cholesterol input, %/week	ND	13.0 (100%)	6.5 (100%)
11	Local biosynthesis	ND	9.4 (72%)	6.3 (97%)
12	Uptake from blood	ND	3.6 (28%)	0.2 (3%)

ND, not determined. Lines in italics represent experimental data; lines in bold indicate the final calculated values, which were determined by using the means of experimental data; ± values represent SD. Animal statistics are indicated in the Materials and Methods.

cholesterol/g wet tissue (Table 1, line 6), then it takes ~54 days (1.13/0.021) to replace the entire retinal cholesterol pool. The rate of cholesterol turnover in this case is 1.85% per day (100%/54 days). Accordingly, for the brain, cholesterol turnover time is ~108 days, and the turnover rate is 0.93% per day.

DISCUSSION

For the first time, the absolute rates of retinal cholesterol biosynthesis and tissue uptake of systemic cholesterol were determined (Table 1, lines 8, 9) revealing that local biosynthesis is the major source of cholesterol for mouse retina. Because animal chow in our study contained 0.3% cholesterol, a lower dietary cholesterol may further increase the quantitative contribution of in situ biosynthesis to total retinal cholesterol input.

Pathways of retinal cholesterol input have been quantified previously in rats. Cholesterol biosynthesis was evaluated after intravitreal injections of the cholesterol precursor [^{3}H]farnesol coinjected with or without the inhibitor of cholesterol biosynthesis NB-598 (7). The determined rate was 46 pmol cholesterol/retina • h or 1.1 nmol/retina • day (7), ~10 times higher than that determined in our study (0.12 nmol/retina • day). A possible reason for this disparity is interspecies differences. Retinal uptake of blood-borne cholesterol was measured in a different study, which utilized intravenous injections of [$^2H_7$] cholesterol-containing LDL (9). This study showed that 2.5% of retinal cholesterol was replaced with [$^2H_7$]cholesterol from LDL in 4 h. This rate is much faster than that (3.6% per week) determined in our work, probably because the former reflects retinal uptake of systemic cholesterol under a heavy LDL load; the amount of injected LDL in this study was high and equal to about half of all animal LDL. In contrast, under normal conditions, serum levels of LDL in rats are low and those of HDL are high.

The retina-brain comparisons demonstrate that in both neural tissues, local biosynthesis is the major source of cholesterol. This is probably because of the blood-brain and blood-retina barriers, respectively, separating the two organs from the systemic circulation. Also, cholesterol biosynthesis is a highly controlled process (25). Accordingly, the brain and retina rely on this process to prevent significant fluctuations of tissue cholesterol. Nevertheless, two quantitative differences between retinal and brain cholesterol input were identified. First, when normalized per gram of wet tissue, the daily rate of total cholesterol input to mouse retina was ~6 times lower than that to mouse brain (21 μg vs. 121 μg). Second, the retina seems to turn cholesterol over more than ~2 times faster than the brain (54 days vs. 108 days). The former difference can be due to a higher cholesterol content in the brain than in the retina (13 mg/g brain vs. 1.13 mg/g retina) even if taking into account that in mice 80% of brain cholesterol is present in myelin sheaths and metabolically inert (26). The latter difference may be apparent because our calculated turnover rates represent an average value for a pool of different, metabolically active cell types present in the two organs. In the brain, neurons, glial cells, and vascular elements almost certainly have very different rates of cholesterol metabolism and turnover (26). Perhaps, the same is true for different retinal cell types. Of importance is that the relative contents of different cell types vary in the brain and retina, and some of these cell types are unique to each organ (e.g., the photoreceptor cells in the retina). Despite this caveat of averaging the turnover rates for different cell types, the calculations of the average cholesterol turnover rates in the brain and retina are useful because they enable a comparison with data obtained previously (10, 27).

Cholesterol input to mouse brain was first characterized by injecting mice intraperitoneally with 50 mCi of tritiated water followed by animal euthanasia 1 h later and the determination of the brain content of ^{3}H-labeled digitonin-precipitated sterols (27). The rate of cholesterol biosynthesis in this study was 0.67%, of which 0.24% was used for brain growth and 0.43% for the turnover because the measurements were conducted in 7-week-old mice, whose pools of cerebral cholesterol were still expanding (28). In our study, the daily rate of cerebral cholesterol biosynthesis was 0.93% (6.3%; Table 1, line 11, divided by 7) and represented the rate in 3- to 4-month-old mice, whose concentrations of brain cholesterol are no longer increasing (27). Our data suggest that a part of cholesterol used for brain growth in young animals becomes available for turnover once mice mature. The previous data also confirm the validity of our approach because similar rates of cholesterol biosynthesis were obtained using two different methods. Thus, a safer approach is now available for the quantifications of tissue cholesterol input based on the use of nonradioactive isotopes. Of interest is to compare the rates of cerebral cholesterol biosynthesis between C57BL/6J mice used herein and heterozygous *Pdgfb*$^{ret/+}$ mice used as a control for mice with disrupted blood brain barrier (the *Pdgfb*$^{ret/ret}$ animals) in our previous study (10). The daily rate of cerebral cholesterol biosynthesis in *Pdgfb*$^{ret/+}$ animals was lower and equal to 0.3% per day.

Local biosynthesis could be an important contributor to cholesterol input to human retina as well because there has been no consistent association between serum cholesterol and AMD (29). Yet, in humans, cholesterol in the systemic circulation is mainly carried by LDL, whereas in mice by HDL. This difference may affect the uptake of systemic cholesterol by human retina and lead to interspecies differences in relative contribution of retinal cholesterol biosynthesis to total cholesterol input. There are additional quantitative and qualitative differences in the way mice and humans handle cholesterol (2). Mice and humans also have differences in retinal architecture and physiology (30) as exemplified by lack of a macula in mice and their inability to naturally develop age-related retinal degeneration. These interspecies differences raise the question of whether our findings in mice can be extrapolated to humans and add new knowledge to the potential use of statins (drugs that inhibit cholesterol biosynthesis) as therapeutics for AMD. Indeed, hallmark manifestations of AMD (drusen and subretinal drusenoid deposits) contain substantial

amounts of cholesterol (31, 32). AMD and retinal cholesterol have also been linked by genetic investigations showing that some cholesterol-related genes (*ABCA1*, *APOE*, *CETP*, and *LIPC*) are risk factors for AMD (33–39).

Studies on retinal effects of statin treatment in animals are scarce and inconsistent. When lovastatin was delivered to rats via a single intravitreal injection, retinal cholesterol biosynthesis was inhibited, yet retinal cholesterol content remained unchanged. Also, there were changes in the retinal cytoarchitecture (40). In contrast, when a different statin (simvastatin) was delivered orally to mice daily for 7 days, retinal cholesterol was decreased (1.4-fold) as was retinal lathosterol (1.3-fold), believed to be a marker for cholesterol biosynthesis (41). Consistent with this work are studies in mice fed a high-fat, atherogenic diet that induced functional changes in the retina and ultrastructural changes in the underlying retinal pigment epithelium and Bruch's membrane (42). Simvastatin treatment of these animals significantly improved retinal function and ultrastructure.

Similar to investigations in animals, studies in humans, largely retrospective or population based in design, produced inconsistent results on retinal effects of statins, namely, on the manifestations of AMD (43, 44). However, recently a prospective randomized controlled trial has been carried out (114 participants) and demonstrated that the cumulative AMD progression rates were lower in the simvastatin-treated group (54%) than in the placebo group (70%) (45). The treatment rate reduction was even more significant when the post hoc analysis was stratified by the baseline AMD severity and *CFH* genotype: >4-fold decrease in people with nonadvanced AMD and >12-fold decrease in carriers of CC (Y402H) *CFH* (45). These promising results suggest that statins should be reconsidered as therapeutics for AMD and that recent studies in simvastatin treatment in mice (41, 42) along with the findings of the present work may be of human relevance.

In summary, the relative and absolute contributions of local biosynthesis and uptake of serum cholesterol to total retinal cholesterol input in mice have been determined and compared with those in the brain. The data obtained are of methodological, fundamental, and clinical significance.

REFERENCES

1. Fliesler, S. J., and R. E. Anderson. 1983. Chemistry and metabolism of lipids in the vertebrate retina. *Prog. Lipid Res.* **22:** 79–131.
2. Pikuleva, I. A., and C. A. Curcio. 2014. Cholesterol in the retina: the best is yet to come. *Prog. Retin. Eye Res.* **41:** 64–89.
3. Pascolini, D., S. P. Mariotti, G. P. Pokharel, R. Pararajasegaram, D. Etya'ale, A. D. Negrel, and S. Resnikoff. 2004. 2002 global update of available data on visual impairment: a compilation of population-based prevalence studies. *Ophthalmic Epidemiol.* **11:** 67–115.
4. Fliesler, S. J., and L. Bretillon. 2010. The ins and outs of cholesterol in the vertebrate retina. *J. Lipid Res.* **51:** 3399–3413.
5. Fliesler, S. J., R. Florman, L. M. Rapp, S. J. Pittler, and R. K. Keller. 1993. In vivo biosynthesis of cholesterol in the rat retina. *FEBS Lett.* **335:** 234–238.
6. Fliesler, S. J., R. Florman, and R. K. Keller. 1995. Isoprenoid lipid metabolism in the retina: dynamics of squalene and cholesterol incorporation and turnover in frog rod outer segment membranes. *Exp. Eye Res.* **60:** 57–69.
7. Fliesler, S. J., and R. K. Keller. 1995. Metabolism of [3H]farnesol to cholesterol and cholesterogenic intermediates in the living rat eye. *Biochem. Biophys. Res. Commun.* **210:** 695–702.
8. Elner, V. M. 2002. Retinal pigment epithelial acid lipase activity and lipoprotein receptors: effects of dietary omega-3 fatty acids. *Trans. Am. Ophthalmol. Soc.* **100:** 301–338.
9. Tserentsoodol, N., J. Sztein, M. Campos, N. V. Gordiyenko, R. N. Fariss, J. W. Lee, S. J. Fliesler, and I. R. Rodriguez. 2006. Uptake of cholesterol by the retina occurs primarily via a low density lipoprotein receptor-mediated process. *Mol. Vis.* **12:** 1306–1318.
10. Saeed, A. A., G. Genove, T. Li, D. Lutjohann, M. Olin, N. Mast, I. A. Pikuleva, P. Crick, Y. Wang, W. Griffiths, et al. 2014. Effects of a disrupted blood-brain barrier on cholesterol homeostasis in the brain. *J. Biol. Chem.* **289:** 23712–23722.
11. Dietschy, J. M., and S. D. Turley. 2001. Cholesterol metabolism in the brain. *Curr. Opin. Lipidol.* **12:** 105–112.
12. Meaney, S., D. Lutjohann, U. Diczfalusy, and I. Bjorkhem. 2000. Formation of oxysterols from different pools of cholesterol as studied by stable isotope technique: cerebral origin of most circulating 24S-hydroxycholesterol in rats, but not in mice. *Biochim. Biophys. Acta.* **1486:** 293–298.
13. Mast, N., R. Reem, I. Bederman, S. Huang, P. L. DiPatre, I. Bjorkhem, and I. A. Pikuleva. 2011. Cholestenoic acid is an important elimination product of cholesterol in the retina: comparison of retinal cholesterol metabolism with that in the brain. *Invest. Ophthalmol. Vis. Sci.* **52:** 594–603.
14. Shah, V., K. Herath, S. F. Previs, B. K. Hubbard, and T. P. Roddy. 2010. Headspace analyses of acetone: a rapid method for measuring the 2H-labeling of water. *Anal. Biochem.* **404:** 235–237.
15. McCabe, B. J., I. R. Bederman, C. Croniger, C. Millward, C. Norment, and S. F. Previs. 2006. Reproducibility of gas chromatography-mass spectrometry measurements of 2H labeling of water: application for measuring body composition in mice. *Anal. Biochem.* **350:** 171–176.
16. Diraison, F., C. Pachiaudi, and M. Beylot. 1996. In vivo measurement of plasma cholesterol and fatty acid synthesis with deuterated water: determination of the average number of deuterium atoms incorporated. *Metabolism.* **45:** 817–821.
17. Lee, W. N., S. Bassilian, H. O. Ajie, D. A. Schoeller, J. Edmond, E. A. Bergner, and L. O. Byerley. 1994. In vivo measurement of fatty acids and cholesterol synthesis using D2O and mass isotopomer analysis. *Am. J. Physiol.* **266:** E699–E708.
18. Lee, W. N., S. Bassilian, Z. Guo, D. Schoeller, J. Edmond, E. A. Bergner, and L. O. Byerley. 1994. Measurement of fractional lipid synthesis using deuterated water (2H2O) and mass isotopomer analysis. *Am. J. Physiol.* **266:** E372–E383.
19. Jones, P. J., C. A. Leitch, Z. C. Li, and W. E. Connor. 1993. Human cholesterol synthesis measurement using deuterated water. Theoretical and procedural considerations. *Arterioscler. Thromb.* **13:** 247–253.
20. Turley, S. D., J. M. Andersen, and J. M. Dietschy. 1981. Rates of sterol synthesis and uptake in the major organs of the rat in vivo. *J. Lipid Res.* **22:** 551–569.
21. Spady, D. K., S. D. Turley, and J. M. Dietschy. 1985. Rates of low density lipoprotein uptake and cholesterol synthesis are regulated independently in the liver. *J. Lipid Res.* **26:** 465–472.
22. Breslow, J. L. 1993. Transgenic mouse models of lipoprotein metabolism and atherosclerosis. *Proc. Natl. Acad. Sci. USA.* **90:** 8314–8318.
23. Peet, D. J., S. D. Turley, W. Ma, B. A. Janowski, J. M. Lobaccaro, R. E. Hammer, and D. J. Mangelsdorf. 1998. Cholesterol and bile acid metabolism are impaired in mice lacking the nuclear oxysterol receptor LXR alpha. *Cell.* **93:** 693–704.
24. Heverin, M., S. Meaney, D. Lutjohann, U. Diczfalusy, J. Wahren, and I. Bjorkhem. 2005. Crossing the barrier: net flux of 27-hydroxycholesterol into the human brain. *J. Lipid Res.* **46:** 1047–1052.
25. Brown, M. S., and J. L. Goldstein. 2009. Cholesterol feedback: from Schoenheimer's bottle to Scap's MELADL. *J. Lipid Res.* **50 (Suppl):** S15–S27.
26. Dietschy, J. M., and S. D. Turley. 2004. Thematic review series: brain Lipids. Cholesterol metabolism in the central nervous system during early development and in the mature animal. *J. Lipid Res.* **45:** 1375–1397.
27. Xie, C., E. G. Lund, S. D. Turley, D. W. Russell, and J. M. Dietschy. 2003. Quantitation of two pathways for cholesterol excretion from the brain in normal mice and mice with neurodegeneration. *J. Lipid Res.* **44:** 1780–1789.

28. Dietschy, J. M., and S. D. Turley. 2002. Control of cholesterol turnover in the mouse. *J. Biol. Chem.* **277:** 3801–3804.
29. Klein, R., C. E. Myers, G. H. Buitendijk, E. Rochtchina, X. Gao, P. T. de Jong, T. A. Sivakumaran, G. Burlutsky, R. McKean-Cowdin, A. Hofman, et al. 2014. Lipids, lipid genes, and incident age-related macular degeneration: the three continent age-related macular degeneration consortium. Am. J. Ophthalmol. 158**:** 513–524.
30. Fliesler, S. J. 2015. Cholesterol homeostasis in the retina: seeing is believing. *J. Lipid Res.* **56:** 1–4.
31. Wang, L., M. E. Clark, D. K. Crossman, K. Kojima, J. D. Messinger, J. A. Mobley, and C. A. Curcio. 2010. Abundant lipid and protein components of drusen. *PLoS One.* **5:** e10329.
32. Oak, A. S., J. D. Messinger, and C. A. Curcio. 2014. Subretinal drusenoid deposits: further characterization by lipid histochemistry. *Retina.* **34:** 825–826.
33. Chen, W., D. Stambolian, A. O. Edwards, K. E. Branham, M. Othman, J. Jakobsdottir, N. Tosakulwong, M. A. Pericak-Vance, P. A. Campochiaro, M. L. Klein, et al.; Complications of Age-Related Macular Degeneration Prevention Trial Research Group. 2010. Genetic variants near TIMP3 and high-density lipoprotein-associated loci influence susceptibility to age-related macular degeneration. *Proc. Natl. Acad. Sci. USA.* **107:** 7401–7406.
34. Neale, B. M., J. Fagerness, R. Reynolds, L. Sobrin, M. Parker, S. Raychaudhuri, P. L. Tan, E. C. Oh, J. E. Merriam, E. Souied, et al. 2010. Genome-wide association study of advanced age-related macular degeneration identifies a role of the hepatic lipase gene (LIPC). *Proc. Natl. Acad. Sci. USA.* **107:** 7395–7400.
35. Klaver, C. C., M. Kliffen, C. M. van Duijn, A. Hofman, M. Cruts, D. E. Grobbee, C. van Broeckhoven, and P. T. de Jong. 1998. Genetic association of apolipoprotein E with age-related macular degeneration. *Am. J. Hum. Genet.* **63:** 200–206.
36. McKay, G. J., C. C. Patterson, U. Chakravarthy, S. Dasari, C. C. Klaver, J. R. Vingerling, L. Ho, P. T. de Jong, A. E. Fletcher, I. S. Young, et al. 2011. Evidence of association of APOE with age-related macular degeneration: a pooled analysis of 15 studies. *Hum. Mutat.* **32:** 1407–1416.
37. Souied, E. H., P. Benlian, P. Amouyel, J. Feingold, J. P. Lagarde, A. Munnich, J. Kaplan, G. Coscas, and G. Soubrane. 1998. The epsilon4 allele of the apolipoprotein E gene as a potential protective factor for exudative age-related macular degeneration. *Am. J. Ophthalmol.* **125:** 353–359.
38. Fritsche, L. G., W. Chen, M. Schu, B. L. Yaspan, Y. Yu, G. Thorleifsson, D. J. Zack, S. Arakawa, V. Cipriani, S. Ripke, et al. 2013. Seven new loci associated with age-related macular degeneration. *Nat. Genet.* **45:** 433–439.
39. Yu, Y., R. Reynolds, B. Rosner, M. J. Daly, and J. M. Seddon. 2012. Prospective assessment of genetic effects on progression to different stages of age-related macular degeneration using multistate Markov models. *Invest. Ophthalmol. Vis. Sci.* **53:** 1548–1556.
40. Pittler, S. J., S. J. Fliesler, P. L. Fisher, P. K. Keller, and L. M. Rapp. 1995. In vivo requirement of protein prenylation for maintenance of retinal cytoarchitecture and photoreceptor structure. *J. Cell Biol.* **130:** 431–439.
41. Zheng, W., N. Mast, A. Saadane, and I. A. Pikuleva. 2015. Pathways of cholesterol homeostasis in mouse retina responsive to dietary and pharmacologic treatments. *J. Lipid Res.* **56:** 81–97.
42. Barathi, V. A., S. W. Yeo, R. H. Guymer, T. Y. Wong, and C. D. Luu. 2014. Effects of simvastatin on retinal structure and function of a high-fat atherogenic mouse model of thickened Bruch's membrane. *Invest. Ophthalmol. Vis. Sci.* **55:** 460–468.
43. Gehlbach, P., T. Li, and E. Hatef. 2009. Statins for age-related macular degeneration. *Cochrane Database Syst. Rev.* **3:** CD006927.
44. Tsao, S. W., and D. S. Fong. 2013. Do statins have a role in the prevention of age-related macular degeneration? *Drugs Aging.* **30:** 205–213.
45. Guymer, R. H., P. N. Baird, M. Varsamidis, L. Busija, P. N. Dimitrov, K. Z. Aung, G. A. Makeyeva, A. J. Richardson, L. Lim, and L. D. Robman. 2013. Proof of concept, randomized, placebo-controlled study of the effect of simvastatin on the course of age-related macular degeneration. *PLoS One.* **8:** e83759.